A Stable Ketene−Pyridine Prereactive Intermediate: Experimental and Theoretical Identifications of the C_3O_2···Pyridine Complex†

Isabelle Couturier-Tamburelli,‡ Jean-Pierre Aycard,*,‡ Ming Wah Wong,§ and Curt Wentrup||

Physique des Interactions Ioniques et Moléculaires, UMR CNRS 6633, Equipe Spectrométries et Dynamique Moléculaire, Université de Provence, Case 542, 13397 Marseille Cedex 20, France, Department of Chemistry, National University of Singapore, Kent Ridge, Singapore 119260, and Department of Chemistry, The University of Queensland, Brisbane, Queensland 4072, Australia

Received: August 26, 1999; In Final Form: December 2, 1999

The structure and energy of the 1:1 pyridine/C_3O_2 complex have been investigated in solid argon matrixes using FTIR spectroscopy as well as ab initio and density functional theory (up to B3LYP/6-311+G(3df,2p)) calculations. Computationally, the complex may exist in a T-shaped form, $\mathbf{T_{Nu}}$, of either C_{2v} or C_s symmetry. The complex trapped in argon matrix is characterized by a large shift of the antisymmetric CCO stretching mode to lower frequency ($\Delta\upsilon = 90$ cm^{-1}). The predicted frequency shifts for the C_{2v} structure of the $\mathbf{T_{Nu}}$ complex are in good agreement with the observed vibrational frequency shifts. This complex is indicative of electrostatic interaction between the nitrogen atom of the pyridine molecule and the C_2 and C_4 atoms of the C_3O_2 moiety (intermolecular bond distance = 3.28 Å). The agreement between calculated and experimental IR spectra together with the calculated structure suggests the presence of a prereactive intermediate of a nucleophilic addition reaction. No stable zwitterionic type structure was observed.

Introduction

The interaction between ketenes and nucleophiles has attracted the attention of many experimental and theoretical chemists.[1] The susceptibility to nucleophilic attack is one of the most characteristic properties of ketenes. These compounds are usually trapped by H_2O or amines to produce acids or amides, respectively. In general, a ketene−nucleophile zwitterion is expected to be formed initially.[2] The reaction with nitrogen nucleophiles giving rise to ketene−amine and ketene−imine zwitterions undoubtedly plays a role in several reactions catalyzed by pyridine or tertiary amines and in the Staudinger reaction between ketenes and imines, leading to β-lactams.[3] In 1996, Wentrup and co-workers observed ketene−pyridine zwitterions directly in cryogenic matrixes.[4] These compounds were characterized by their strong infrared absorption bands around 1680 cm^{-1}. Theoretical calculations at ab initio (HF/6-31G*) and DFT (BLYP and B3LYP/6-31G*) levels indicate the initial formation of a molecular complex, followed by the formation of the zwitterion, whereby the latter has a very low barrier toward dissociation in the gas phase but can be stabilized very significantly in the presence of a dielectric (i.e., solvent) field. There is a corresponding shortening of the pyridine−ketene bond when going from the gas phase to the solvated zwitterion.[4b,5]

Previous experiments in our laboratory have shown that the parent bisketene, carbon suboxide (C_3O_2), is a substrate of choice for the investigation of structure, energy, and reactivity of the 1:1 complex with both electrophiles[6] and nucleophiles.[7]

The purpose of the present work was to obtain direct and accurate experimental results on the C_3O_2···pyridine complex trapped in a cryogenic matrix.

Experimental Section

Pure C_3O_2 was synthesized using the method described by Long et al.[8] Pyridine was supplied by Prolabo (France) and distilled over KOH before use.

Gas mixtures of C_3O_2/Ar, pyridine/Ar, and C_3O_2/pyridine/Ar with ratios 1/500, 10/500, and 1/10/500, respectively, were prepared by standard manometric techniques and deposited on a CsBr window at 20 K. The deposition rate (2 mmol/h) of the gas mixtures was controlled with an Air Liquide microleak (VP/RX). A Nicolet 7199 FTIR spectrometer was used to record the spectra of samples cooled to 10 K in the range 400−4000 cm^{-1} with a resolution of 0.12 cm^{-1}.

Results and Discussion

Argon matrixes containing only C_3O_2 or pyridine yielded IR absorption spectra as indicated in Figure 1 and Table 1. These are in agreement with previous observations, and the spectral assignments are based upon the works of Pietri et al.,[6a,b] for C_3O_2, and Carpenter et al.[9a] and Tevault et al.,[9b] for pyridine.

A. The C_3O_2/pyridine/Ar Matrix. *A.1. Infrared Absorption Spectra.* The spectra recorded at 10 K after co-deposition of C_3O_2/pyridine/Ar show new absorption bands (Figure 1b), marked with an asterisk in the figure, with respect to the spectra of pure C_3O_2[6a,b] (Figure 1a) and pure pyridine (Figure 1c) in argon matrixes (Table 1). In the ν_{CCO} region between 2400 and 2100 cm^{-1} (ν_3 and ν_1), we observe the characteristic absorption bands of the C_3O_2 monomer (Figure 2; antisymmetric ν_{CCO} and symmetric ν_{CCO} at 2289.3 and 2194.4 cm^{-1}, respectively). Both modes exhibit multiple absorption lines due to different matrix sites. Thus, additional sites are seen at 2270 and 2190 cm^{-1} in Figures 1 and 2. The most intense band of the ν_{as} mode of C_3O_2 in the presence of pyridine appears at 2199.3 cm^{-1} (Figure 2). This value is shifted toward lower frequencies by 90 cm^{-1} with respect to the most intense component of the ν_{as} absorption band of C_3O_2 monomer.

† Part of the special issue "Marilyn Jacox Festschrift".
‡ Université de Provence.
§ National University of Singapore.
|| University of Queensland.

10.1021/jp9930548 CCC: $19.00
Published on Web 01/26/2000

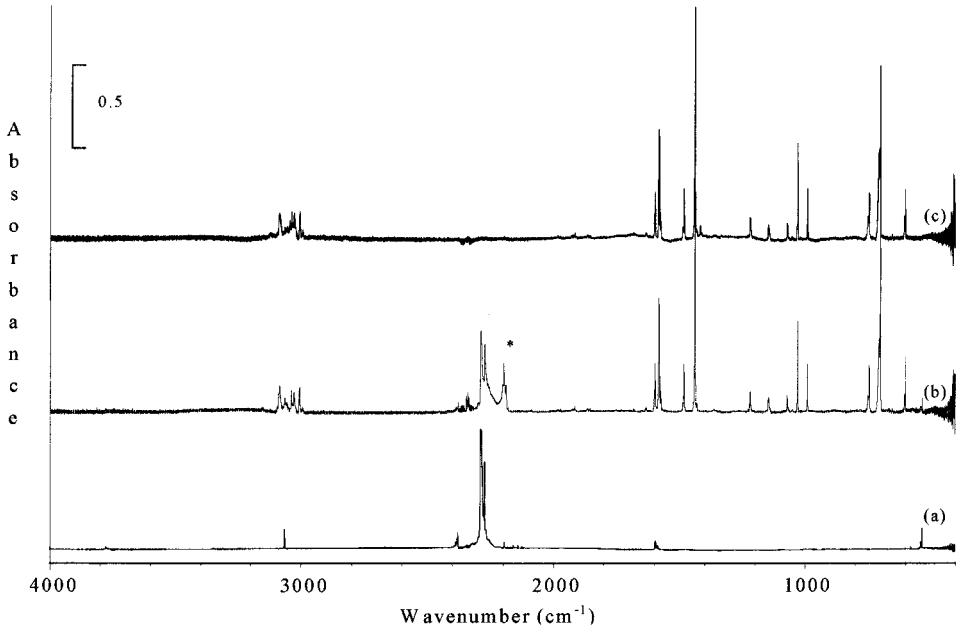

Figure 1. Infrared spectra of C_3O_2, pyridine, and the C_3O_2/pyridine complex isolated in argon matrix at 10 K, in the 4000−400 cm^{-1} range: (a) C_3O_2/Ar in the ratio 1/500; (b) C_3O_2/pyridine/Ar in the ratio 1/10/500; (c) pyridine/Ar in the ratio 10/500.

TABLE 1: Experimental and Calculated C_3O_2 Frequency Shifts in the C_{2v} C_3O_2/Pyridine Complex ($\Delta\nu = \nu_{isolated} - \nu_{complexed}$)

	ν (cm^{-1})												$\Delta\nu$ (cm^{-1})		
	experiment				HF/6-31G*				B3LYP/6-31G*					calculated	
mode	isolated C_3O_2	I^a	$\mathbf{T_{Nu}}$ C_{2v} complex	I^a	isolated C_3O_2	I^a	$\mathbf{T_{Nu}}$ C_{2v} complex	I^a	isolated C_3O_2	I^a	$\mathbf{T_{Nu}}$ C_{2v} complex	I^a	exptl	HF	B3LYP
as ν_{CCO}	2289.3	100.0	2199.3	100.0	2463.1	100.0	2379.9	100.0	2423.1	100.0	2342.0	100.0	90.0	83.2	81.1
s ν_{CCO}	2194.4	1.9	2190.5	1.7	2474.9	0.0	2443.8	5.5	2278.0	0.0	2270.0	3.6	3.9	31.1	8.0
ν_{CC}	1596.3	4.2			1808.4	1.1	1701.6	0.6	1650.9	3.6	1594.5	0.3		106.8	56.4
ν_5'	577.0	0.0	570.2	0.7	680.6	0.0	674.5	0.0	582.8	0.0	574.0	3.2	7.2	6.1	8.8
ν_6	538.5	0.2			671.9	3.0	658.2	4.1	577.2	2.6	567.3	0.0		13.7	9.9
ν_6'	532.8	2.7			671.8	3.0	650.1	0.5	577.1	2.6	563.1	4.8		21.7	14.0

[a] Intensity in percent (%) relative to that of the antisymmetric CCO stretching vibration.

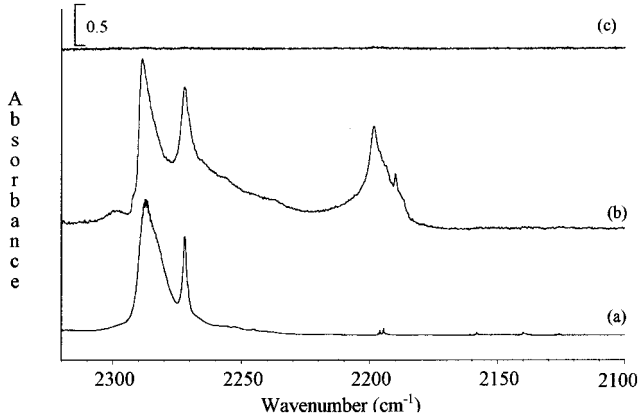

Figure 2. Infrared spectra of C_3O_2, pyridine, and the C_3O_2/pyridine complex isolated in argon matrix at 10 K, in the 2320−2100 cm^{-1} range: (a) C_3O_2/Ar in the ratio 1/500; (b) C_3O_2/pyridine/Ar in the ratio 1/10/500; (c) pyridine/Ar in the ratio 10/500.

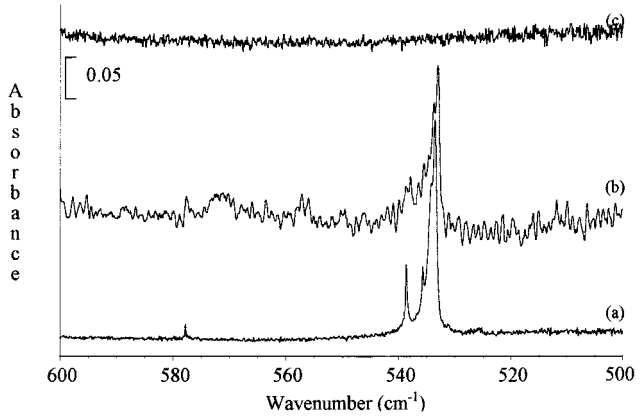

Figure 3. Infrared spectra of C_3O_2, pyridine, and the C_3O_2/pyridine complex isolated in argon matrix at 10 K, in the 600−500 cm^{-1} range: (a) C_3O_2/Ar in the ratio 1/500; (b) C_3O_2/pyridine/Ar in the ratio 1/10/500; (c) pyridine/Ar in the ratio 10/500.

Another characteristic feature in the spectrum is the evolution of the symmetric ν_{CCO} vibrational mode. This appears at 2190.5 cm^{-1} in the C_3O_2/pyridine/Ar matrix and is shifted less than the antisymmetric mode ($\Delta\upsilon = 3$ cm^{-1}), but its intensity is strongly increased. Such an effect was also observed for the complexes C_3O_2···NH_3 and C_3O_2···H_2O.[7] This fact suggests a high degree of distortion of the C_3O_2 moiety complexed with pyridine with respect to the monomer. A very weak band in the bending vibrational region at 570.2 cm^{-1} may be due to $\nu_{5'}$ of C_3O_2 (Figure 3 and Table 1). The infrared spectrum of pyridine was essentially unchanged in the presence of C_3O_2.

The spectral features described above and the agreement with the calculated spectrum (see below) are indicative of the formation of a prereactive intermediate complex between C_3O_2 and pyridine.

A.2. Annealing Experiments. Warmup of the matrix above 40 K induces changes in the IR spectra without apparition of

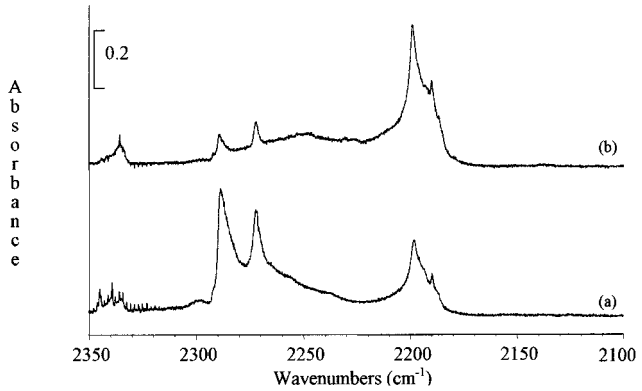

Figure 4. Effect of annealing of the C_3O_2/pyridine mixture on the IR spectrum in the symmetric and antisymmetric ν_{CCO} region: (a) C_3O_2/pyridine/Ar in the ratio 1/10/500 at 10 K; (b) C_3O_2/pyridine/Ar in the ratio 1/10/500 at 10 K after annealing to 40 K.

any bands that could be ascribed to a ketene−pyridine zwitterion. In the ν_3 mode region, we observe an increase in intensity of the $C_3O_2\cdots$pyridine complex bands in concert with a decrease in that of the monomer ones (Figure 4). Bands due to pyridine decrease at the same time. The most probable explanation is a reorganization of the trapping sites when the temperature is raised. This allows diffusion in the matrix and the formation of more complexes, but still without any formation of zwitterions.

A.3. Other Matrixes and Experiments. Several other experiments were carried out in an effort to obtain the $C_3O_2\cdots$pyridine zwitterion. First, matrixes with different C_3O_2/pyridine/Ar ratios were prepared. A pure pyridine−C_3O_2 matrix was also formed. In all these experiments, the same absorption bands, corresponding to the $C_3O_2\cdots$pyridine complex, appear. Second, warming of the pyridine−C_3O_2 matrix above 200 K, or depositing this mixture at 77 K, revealed only the formation of the absorption bands ascribed to the complex.

B. Structure and Bonding in the $C_3O_2\cdots$Pyridine Complex. Several geometric arrangements are possible for the pyridine and C_3O_2 subunits in the complex. On the basis of results obtained for the $C_3O_2\cdots NH_3$ complex, the nitrogen atom of pyridine is expected to attack carbon suboxide on the C_α atom of the ketene moiety.[7] This is supported by calculated atomic charges of C_3O_2, based on the natural bond orbital (NBO)[10] analysis: $C_\alpha = +0.71$, $C_\beta = -0.57$, and $O = -0.42$ (B3LYP/6-31G*). Thus, the structure for consideration is the $\mathbf{T_{Nu}}$ complex,[7] which can exist in either C_{2v} or C_s forms (Scheme 1).

To establish the possible molecular structures of the $C_3O_2\cdots$pyridine complexes, ab initio and density functional calculations were carried out using the Gaussian 94 package,[11] first with the Hartree−Fock (HF) method and subsequently with the B3LYP[12] DFT procedure, using the split-valence polarized 6-31G* basis set. Geometry was fully optimized at these levels of theory. Harmonic vibrational frequencies were determined at the optimized geometries and compared with experimental data (Table 1). The structures of the two $\mathbf{T_{Nu}}$ complexes are characterized by three independent variables R, α, and β (cf. Scheme 1), denoting the distance between the pyridine nitrogen atom and C_α of the carbon suboxide, the intermolecular angle between R and the C_3O moiety of carbon suboxide, and the angle between R and the N−C bond of pyridine, respectively.

On the HF/6-31G*potential energy surface, only one minimum was located for the values $R = 3.293$ Å, $\alpha = 91.9°$, and $\beta = 100.0°$, corresponding to the planar C_{2v} $\mathbf{T_{Nu}}$ structure (Scheme 2). The C_3O_2 moiety of this C_{2v} complex is strongly

SCHEME 1: Two Kinds of $C_3O_2\cdots$Pyridine Interaction Leading to the C_{2v} $\mathbf{T_{Nu}}$ and C_s $\mathbf{T_{Nu}}$ Complex Structures with Numbering of the Subunits[a]

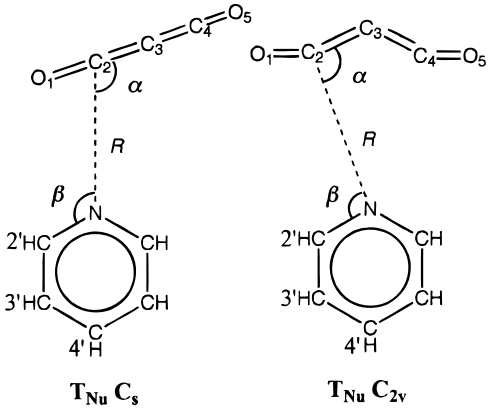

[a] The geometrical parameters, distance R, and angles α and β are defined in the text.

bent ($\angle CCC = 134.0°$), and the C=C bond is slightly lengthened by 0.014 Å (Table 2).

On the B3LYP energy surface, we obtain two local minima (Scheme 2). The first minimum has the values $R = 3.282$ Å, $\alpha = 78.0°$, and $\beta = 99.5°$, corresponding to the C_{2v} $\mathbf{T_{Nu}}$ complex. Its geometry is similar to the HF one except for a significantly wider CCC angle (142.3°). The CCC and the CCO valence bond angles in the C_{2v} complex correspond to a change of hybridization of the central carbon atom from sp t*o* sp^2. It is important to note that the bending potential of the C_3O_2 is extremely flat.[13] The calculated CCC bending frequency is just 47 cm^{-1}, and the energy difference between the equilibrium structure and the bent structure with $\angle CCC = 142°$ is only 6.7 kJ mol^{-1} (B3LYP/6-31G*). The energy required to bend the C_3O_2 subunit in the $\mathbf{T_{Nu}}$ C_{2v} complex is more than compensated by the two favorable $N\cdots C_\alpha$ donor−acceptor interactions (see below).

The second minimum, at the B3LYP level, corresponds to the C_s $\mathbf{T_{Nu}}$ structure ($R = 3.095$ Å, $\alpha = 98.1°$, and $\beta = 108.2°$). The geometry of the C_s complex (Scheme 2) is totally different from that of the C_{2v} one. The pyridine and C_3O_2 moieties are coplanar, but the C_3O_2 moiety is almost linear. The $N\cdots C$ distance R is shorter than that in the C_{2v} form by 0.20 Å. At the B3LYP/6-31G* level, the C_s complex is more stable than the C_{2v} structure by just 1.2 kJ mol^{-1}. However, at the higher level B3LYP/6-311+G(3df,2p) and including zero-point energy (ZPE) correction, the preferred structure of the $C_3O_2\cdots$pyridine complex is the C_{2v} form. We have examined the basis set superposition error (BSSE) of the stabilities of the $\mathbf{T_{Nu}}$ complexes using the counterpoise method[14] and found the influence of BSSE is very small. The $\mathbf{T_{Nu}}$ C_{2v} complex is predicted to be stable with respect to the monomers by 3.6 kJ mol^{-1} (Table 3). The structure of the C_{2v} complex is similar to that of the $C_3O_2\cdots NH_3$ complex but lacks the distortion of the latter.[7]

The values of the calculated structural parameters and of the vibrational frequencies, for the free and complexed molecules, are reported in Tables 2 and 1, respectively. Examination of Table 1 shows inversions between the symmetric and antisymmetric CCO stretching frequencies at the HF/6-31G* level. With the B3LYP method these calculated values appear in the correct sequence. To identify the form presents in argon matrixes, it is therefore appropriate to compare the experimental C_3O_2 frequency shifts in the complex with those calculated by the DFT method (Table 1). Examination of these data shows good

SCHEME 2: Optimized Geometries (B3LYP/6-31G*) for the C_3O_2···Pyridine Complexes and Zwitterion (Bond Lengths in Angstroms and Angles in Degrees)

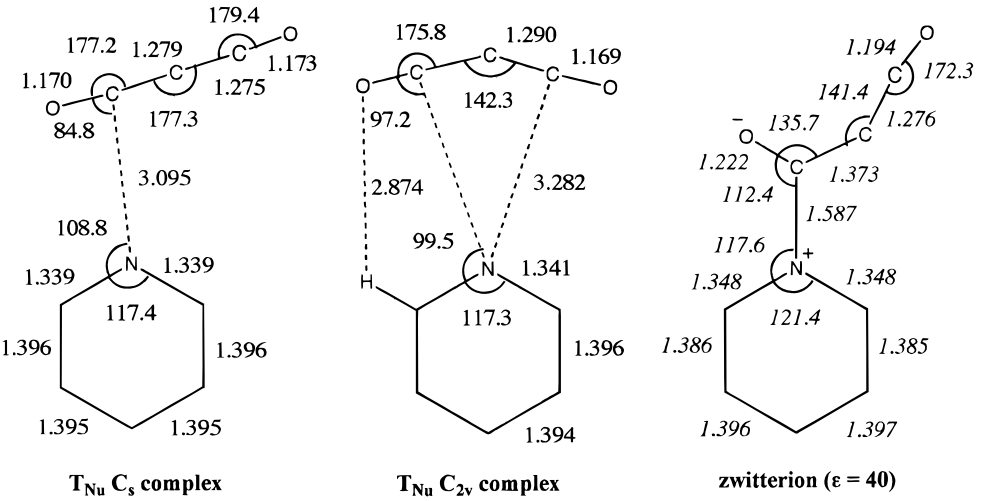

T_{Nu} C_s complex | T_{Nu} C_{2v} complex | zwitterion (ε = 40)

TABLE 2: Optimized Structural Parameters for the Individual Monomers and T_{Nu} Complexes (Bond Length in Angstroms and Angle in Degrees)[a]

	C_3O_2/pyridine monomer		T_{Nu} C_{2v} complex		T_{Nu} C_s complex[b]
parameters	HF/ 6-31G*	B3LYP/ 6-31G*	HF/ 6-31G*	B3LYP/ 6-31G*	B3LYP/ 6-31G*
$r(C_2O_1)$	1.140	1.170	1.138	1.169	1.170
$r(C_2C_3)$	1.268	1.278	1.286	1.290	1.279
$r(C_3C_4)$	1.268	1.278	1.286	1.290	1.275
$r(C_4O_5)$	1.140	1.170	1.138	1.169	1.173
$\angle O_1C_2C_3$	179.9	180.0	175.3	175.8	177.2
$\angle C_2C_3C_4$	177.2	177.2	134.0	142.3	177.3
$\angle C_3C_4O_5$	179.9	180.0	175.3	175.8	179.4
r(NC2′)	1.321	1.340	1.322	1.341	1.339
r(C2′C3′)	1.385	1.396	1.385	1.396	1.396
r(C3′C4′)	1.384	1.394	1.394	1.394	1.395
α			91.9	87.0	98.1
β			100.0	99.5	108.2
R			3.293	3.282	3.095

[a] B3LYP/6-31G* total energies: −248.28496 (pyridine), −264.71993 (C_3O_2), −513.00820 (T_{Nu} C_{2v}), and −513.00864 (T_{Nu} C_s) hartrees. [b] The T_{Nu} C_s complex does not exist at the HF/6-31G* level, collapsing without a barrier to the C_{2v} complex upon geometry optimization.

agreement between the experimental and calculated frequency shifts for the T_{Nu} C_{2v} complex. In particular, the observed frequency shift (90 cm^{-1}) of the asymmetric CCO stretching mode is well reproduced by theory. A calculation of the IR spectrum of C_3O_2 with a CCC angle constrained to 160° demonstrates that such an angle causes an increased intensity of the symmetric ν_{CCO} absorption band and a larger frequency shift of the antisymmetric one, as observed. In contrast, the corresponding frequency shift in the C_s complex is very small (5.8 cm^{-1}; Table 4). Thus, it is confirmed that the observed C_3O_2···pyridine complex has the C_{2v} rather than the C_s structure.

The bonding in the complex is best described in terms of electrostatic attraction of the van der Waals type. NBO charge density analysis at the B3LYP/6-31G* level reveals that the pyridine N atom bears a strong negative charge (−0.48), while the C_α atoms of the C_3O_2 subunit bear a strong positive charge (0.72). There is no bond critical point between the two atoms. Thus, Coulombic attraction is probably the main factor stabilizing the C_{2v} complex. CH···O hydrogen bonding helps to stabilize the planar structure of the complex. The distance between the oxygen and the hydrogen atom in position 2 of the pyridine ring (H(C2′)) is 2.874 Å, shorter than the sum of their van der Waals radii (3.05 Å). The O−C2′ distance is 3.653 Å. The C2′−H stretching vibration is shifted to higher wavenumbers by 10 cm^{-1} in the complex. The electron population at H(C2′) has decreased by 0.005, while that at O is increased by 0.013 electrons. These data are similar to recently calculated ones[15] for CH···O hydrogen bonding and indicate a significant (but not strong) CH···O type of interaction. No minimum was found for a perpendicular conformer (i.e., pyridine and C_3O_2 in perpendicular planes), and this structure is about 2.3 kJ mol^{-1} higher in energy. Thus, the CH···O bonding is worth ca. 1 kJ mol^{-1} per hydrogen bond, and this interaction persists in the presence of a polar dielectric medium ($\epsilon = 40$, using the SCRF dipolar solvation model[16]).

C. Mechanism of Zwitterion Formation. Density functional calculations at the B3LYP/6-311+G**//B3LYP/6-31G* + ZPE level were used to study the mechanism of formation of a C_3O_2−pyridine zwitterion in the gas phase (dielectric constant $\epsilon = 1$) and in a polar medium[16] ($\epsilon = 40$). No stable zwitterionic structure was found on the gas-phase potential energy surface. However, a stable equilibrium structure was located in a polar medium ($\epsilon = 40$). The optimized geometry of the zwitterion is given in Scheme 2. The zwitterion has a planar structure and is characterized by an N−(CO) bond distance of 1.587 Å, significantly longer than a typical N−C single bond (1.38 Å).[17] For the CO and CCO moieties, the bond distances and angles correspond to those of carbonyl and ketene functional groups (Scheme 2). The distortion of the zwitterion geometry compared to the C_{2v} complex results in a dramatic change in the C═C═O stretching vibration from 2342.4 cm^{-1} in the complex to 2186.0 cm^{-1} in the zwitterion. The calculated B3LYP/6-31G* (unscaled) vibrational frequencies are listed in Table 4. The zwitterion is planar, and the H(C2′)···O hydrogen bonding is particularly strong in this case, causing a short O···H distance (2.223 Å) and a large blue shift (97 cm^{-1}) of the C2′−H stretching vibration.

How stable is the zwitterion? It is predicted to lie 28.0 kJ.mol^{-1} above the T_{Nu} C_{2v} complex and 23.9 kJ.mol^{-1} above the monomers (B3LYP/6-311+G** + ZPE, SCIPCM[11,18] solvation model) (Table 3). Dissociation to the C_3O_2 and pyridine monomers is associated with a small activation barrier of just 4.3 kJ mol^{-1}. Hence, our calculation predicts the zwitterion not to be an experimentally accessible species. Even condensation of C_3O_2 and pyridine at 77 K does not appear to

TABLE 3: Calculated Total and Relative Energies[a]

	total energy (hartrees)		ZPE[b] (hartrees)		relative energy (kJ mol^{-1})	
	$\epsilon = 1$	$\epsilon = 40$[c]	$\epsilon = 1$	$\epsilon = 40$[c]	$\epsilon = 1$	$\epsilon = 40$[c]
C_3O_2	−264.82258	−264.82515	0.02184	0.02160		
pyridine	−248.36888	−248.37017	0.08903	0.08905		
$\mathbf{T_{Nu}}$ C_{2v} complex	−513.19339	−513.19765	0.11145	0.11142	−3.6	−4.1
$\mathbf{T_{Nu}}$ C_s complex	−513.19342	−513.19775	0.11174	0.11167	−2.9	−3.8
zwitterion	*d*	−513.18950	*d*	0.11399	*d*	23.9
zwitterion T. S.	*d*	−513.18595	*d*	0.11205	*d*	28.2
C_3O_2 + pyridine	−513.19146	−513.19532	0.11086	0.11066	0.0	0.0

[a] B3LYP/6-311+G(3df,2p)//B3LYP/6-31G* + ZPE level. [b] B3LYP/6-31G* values, scaled by 0.9804 for zero-point energy correction. [c] SCIPCM solvation model, based on the SCRF (dipole) geometry. [d] The zwitterion does not exist in the isolated state ($\epsilon = 1$).

TABLE 4: Calculated (Unscaled) B3LYP/6-31G* Vibrational Frequencies

species	vibrational frequency (cm^{-1})										
C_3O_2	123.1	577.1	577.2	582.8	585.5	788.3	1650.9	2278.1	2423.1		
pyridine	386.2	421.3	613.7	670.2	718.5	762.9	897.8	956.7	993.8	1009.6	1011.8
	1051.2	1086.9	1100.4	1181.3	1253.1	1307.9	1397.9	1487.7	1530.7	1637.8	1644.6
	3169.4	3171.6	3191.6	3207.3	3215.5						
$\mathbf{T_{Nu}}$ C_{2v} complex	6.2	29.5	30.2	48.7	57.2	83.6	132.2	389.8	422.3	563.1	567.3
	574.0	578.3	617.6	669.4	721.4	764.6	890.2	900.1	965.1	1001.3	1013.2
	1015.1	1050.9	1088.4	1100.7	1182.4	1255.9	1308.0	1400.3	1488.5	1532.3	1594.5
	1637.1	1647.1	2270.0	2342.4	3180.7	3181.7	3194.9	3210.6	3218.1		
$\mathbf{T_{Nu}}$ C_s complex	18.5	24.3	33.4	57.2	67.3	131.1	148.0	389.5	421.7	565.6	579.5
	579.8	591.6	616.2	669.8	720.3	764.2	788.3	899.7	961.7	998.6	1012.5
	1014.4	1050.5	1087.7	1100.7	1182.0	1252.8	1310.2	1397.2	1488.3	1531.2	1638.1
	1645.8	1647.8	2274.1	2417.3	3171.0	3182.3	3192.8	3208.5	3216.2		
zwitterion[a]	56.2	80.0	111.8	176.3	239.7	309.5	415.4	433.9	444.8	551.3	606.8
	659.2	665.0	686.6	690.0	717.0	805.5	899.3	928.8	1002.7	1014.9	1039.3
	1048.5	1062.2	1084.6	1113.6	1198.9	1222.0	1351.8	1374.4	1486.6	1511.0	1529.3
	1626.1	1668.3	1829.7	2186.0	3224.8	3231.2	3240.8	3244.0	3267.8		

[a] In a dielectric medium of $\epsilon = 40$ (SCRF dipole model).

SCHEME 3: Reactions between C_3OX Molecules and Nucleophiles

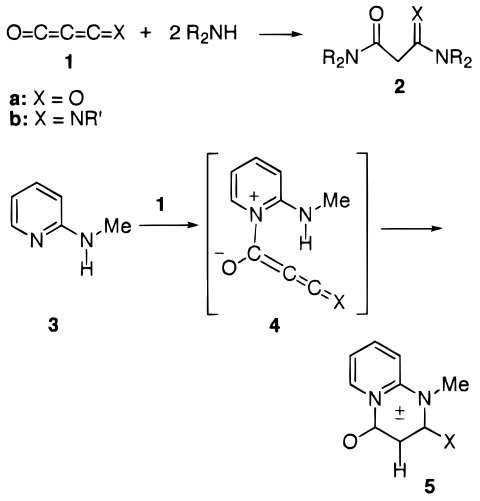

give the zwitterion. Subsequent warming of this matrix leads to evaporation of the components.

D. Further Reaction: Outlook. How can one understand the formation of a complex but lack of a zwitterion? Does no chemical reaction take place? Yes, it does, but at much higher temperatures when the endothermicity of zwitterion formation can be overcome and an overall exothermic reaction can take place. Thus, it is known that C_3O_2 (**1a**) reacts slowly at room temperature with water to produce malonic acid, and more rapidly with amines to afford malonamides (**2a**) (Scheme 3).[19] A previous paper from our laboratory reported the matrix isolation of C_3O_2/water and C_3O_2/ammonia complexes, which are the assumed pre-reactive intermediates en route to malonic acid and malonamide.[7] We have studied the analogous reaction of iminopropadienones (**1b**) elsewhere (Scheme 3) and found that reaction with secondary amines takes place at temperatures above −100 °C to form amidoketenimines **3** as the first observed products, by addition of the nucleophile to the C═O moiety. Importantly, the iminopropadienones can be observed in the presence of amines at ca. −100 °C.[20] Moreover, both **1a** and **1b** react with 2-aminopyridines at room temperature to form mesoionic heterocycles **5**.[19,21] In the case of **1b**, we know that the CCO moiety is far more reactive than the CCN moiety. The structure of the product **5** reveals that the first step of the reaction involves the interaction of the pyridine ring nitrogen with the ketene function. This would take place via reversible formation of van der Waals complexes and then zwitterion **4**. The second step is the reaction of the exocyclic amino group with the C═C═N function in zwitterion **4**. This leads to the product **5** in an exothermic and irreversible reaction. In the reaction studied in this paper we have only observed the first step, the van der Waals complex formation, because no thermodynamically stable product can be formed. In the reaction between pyridine and simple ketenes, the zwitterions are marginally more stable (of lower free energy) than the van der Waals complexes and hence can be observed at low temperatures,[4] but dissociate again at higher temperatures[4b,5b] unless an irreversible reaction can take place.

Conclusions

Deposition of a C_3O_2/pyridine/Ar mixture at cryogenic temperatures affords a molecular complex, which can be termed a prereactive intermediate of a nucleophilic addition reaction. In conjunction with DFT calculations, the magnitude of the frequency shifts of the C_3O_2 vibrational modes is indicative of the formation of a C_{2v} $\mathbf{T_{Nu}}$ complex, resulting from an

electrostatic van der Waals type interaction between the pyridine nitrogen atom and the C_2 and C_4 carbon atoms of the C_3O_2 moiety.

Acknowledgment. This work was supported by the CNRS, the National University of Singapore (Grant 3981643) and the Australian Research Council.

References and Notes

(1) (a) Tidwell, T. T. *Ketenes*; Wiley-Interscience: New York, 1995; p 571. (b) Wentrup, C.; Heilmayer, W.; Kollenz, G. *Synthesis* **1994**, 1218.

(2) Pacansky, J.; Chang, J. S.; Brown, D. W.; Scharwz, W. *J. Org Chem.* **1982**, *47*, 2233. Barra, M.; Fisher, T. A.; Cerrigliaro, Sinta, R.; Scaiano, J. C. *J. Am. Chem. Soc.* **1992**, *114*, 2630. Andraos, J.; Kresge, A. J. *J. Am. Chem. Soc.* **1992**, *114*, 5643. Chelain, E.; Goumont, R.; Hamon, L.; Parlier, A.; Rudler, M.; Rudler, H.; Daran, J.-C.; Vaissermann, J. *J. Am. Chem. Soc.* **1992**, *114*, 8088. Wang, J. L.; Toscano, J. P.; Platz, M. S.; Nikolaev, V.; Popik, V. *J. Am. Chem. Soc.* **1995**, *117*, 7, 5477. Chiang, Y.; Kresge, A. J.; Popik, V. V. *J. Am. Chem. Soc.* **1999**, *121*, 5930.

(3) Palomo, C.; Cossio, F. P.; Odiozola, J. M.; Ioarbide, M.; Ontoria, J. M. *J. Org. Chem.* **1991**, *56*, 6, 4418. Fang, D. C.; Fu, X. Y. *Int. J. Qantum Chem*. **1992**, *43*, 669. Cossio, F. P.; Ugalde, J. M.; Lopez, X.; Lecea, B.; Palomo, C. *J. Am. Chem. Soc.* **1993**, *115*, 995. Cossio, F. P.; Arrieta, A.; Lecea, B.; Ugalde, J. M. *J. Am. Chem. Soc.* **1994**, *116*, 2085. Fang, D. C.; Fu, X. Y. *Int. J. Qantum Chem*. **1996**, *57*, 1107. Lopez, R.; Ruiz-Lopez, M. F.; Rinald, D. *J. Phys. Chem.* **1996**, *100*, 10600. Suarez, F.; Sordo, T. L. *J. Am. Chem. Soc.* **1997**, *119*, 10291. Bibas, H.; Koch, R.; Wentrup, C. *J. Org. Chem.* **1998**, *63*, 2619.

(4) (a) Qiao, G. G.; Andraos, J.; Wentrup, C. *J. Am. Chem. Soc.* **1996**, *118*, 5634. (b) Visser, P.; Zuhse, R.; Wong, M. W.; Wentrup, C. *J. Am. Chem. Soc.* **1996**, *118*, 12598.

(5) (a) Fang, D. C.; Fu, X. Y. *J. Mol. Struct. (THEOCHEM)* **1998**, *455*, 59. (b) Kollenz, G.; Holzer, S.; Dalvi, T. S.; Kappe, C. O.; Fabian, W.; Wong, M. W.; Wentrup, C. Unpublished results.

(6) (a) Pietri, N.; Chiavassa, T.; Allouche, A.; Aycard, J. P. *J. Phys. Chem. A* **1997**, *101*, 1093. (b) Pietri, N. Thesis, Université de Provence, Marseille, 1996.

(7) Couturier-Tamburelli, I.; Chiavassa, T.; Aycard, J. P. *J. Am. Chem. Soc.* **1999**, *121*, 3756.

(8) Long, D. A.; Murfin, F. S.; Williams, R. L. *Proc. R. Soc.* **1954**, *A223*, 251.

(9) (a) Carpenter, J. D.; Ault, B. S. *J. Phys. Chem*. **1993**, *97*, 11397. (b) Tevault, D. E.; Smardzewki, R. R. *J. Chem. Phys.* **1982**, *77*, 2221.

(10) Reed, A. E.; Curtiss, L. A.; Weinhold, F. *Chem. Rev*. **1988**, *88*, 899.

(11) Frisch, M. J.; Trucks, G. W.; Schlegel, H. B.; Gill, P. M. W.; Johnson, B. G.; Robb, M. A.; Cheeseman, J. R.; Keith, T.; Petersson, G. A.; Montgomery, J. A.; Raghavachari, K.; Al-Laham, M. A.; Zakrzewski, V. G.; Ortiz, J. V.; Foresman, J. B.; Cioslowski, J.; Stefanov, B. B.; Nanayakkara, A.; Challacombe, M.; Peng, C. Y.; Ayala, P. Y.; Chen, W.; Wong, M. W.; Andres, J. L.; Replogle, E. S.; Gomperts, R.; Martin, R. L.; Fox, D. J.; Binkley, J. S.; Defrees, D. J.; Baker, J.; Stewart, J. P.; Head-Gordon, M.; Gonzalez, C.; Pople, J. A. *Gaussian 94*; Gaussian, Inc.: Pittsburgh, PA, 1995.

(12) (a) Becke, A. D. *J. Chem. Phys*. **1993**, *98*, 5648. (b) Lee, C.; W. Yang, W.; Parr, R. G. *Phys. Rev. B* **1988**, *37*, 785.

(13) Pyykkö, P.; Runeberg, N. *J. Mol. Struct. (THEOCHEM*) **1991**, *234*, 279. Amos, R. D. *Chem. Phys. Lett.* **1984**, *108*, 347. Jensen, P.; Johns, J. W. C. *J. Mol. Struct.* **1986**, *118*, 248.

(14) Boys, S.; Bernardi, F. *Mol. Phys*. **1970**, *19*, 553.

(15) Gu, Y.; Kar, T.; Scheiner, S. *J. Am. Chem. Soc.* **1999**, *121*, 9411.

(16) (a) Wong, M. W.; Frisch, M. J.; Wiberg, K. B. *J. Am. Chem. Soc*. **1991**, *113*, 4776. (b) Wong, M. W.; Wiberg, K. B.; Frisch, M. J. *J. Chem. Phys*. **1991**, *95*, 8991.

(17) Allen, F. H.; Kennard, O.; Wattson, D. G.; Brammer, L.; Orpen, A. G.; Taylor, R. *J. Chem. Soc., Perkin Trans. 2* **1987**, 1.

(18) Wiberg, K. B.; Keith, T. A.; Frisch, M. J.; Murcko, M. *J. Phys. Chem*. **1995**, *99*, 7702.

(19) Kappe, T.; Ziegler, E. *Angew. Chem., Int. Ed. Engl.* **1974**, *13*, 491.

(20) (a) Wentrup, C.; Rao, V. V. R.; Frank, W.; Fulloon, B. E.; Moloney, D. W. J.; Mosandl, T. *J. Org. Chem.* **1999**, *64*, 3608. (b) Plüg, C.; Frank, W.; Wentrup, C. *J. Chem. Soc., Perkin Trans. 2* **1999**, 1087.

(21) Wentrup, C.; Bibas, H.; Neumann, R.; Shtaiwi, M. Unpublished results.